

Flow front tracking in ALE/Eulerian formulation FEM simulations of aluminium extrusion.

A.J. Koopman^{1,a}, H.J.M. Geijselaers^{1,b}, J. Huétink^{1,c}

¹University of Twente, P.O. Box 217, 7500 AE Enschede, The Netherlands

^aA.J.Koopman@utwente.nl, ^bH.J.M.Geijselaers@utwente.nl, ^cJ.Huetink@utwente.nl

Keywords: Simulation, Finite Element Method, Pseudo Concentration, Filling

Abstract: Even though Extrusion is often regarded as a semi stationary process, the deformations of the die at the beginning of the process can have great influence on the process later on. During filling of the die, the deformation of the die depends on the location of the flow front up to a point where parts of the profile will be opened or closed, especially in porthole dies. In this paper we present an accurate 2D method to simulate the filling of extrusion dies. The method is based on the pseudo concentration technique. We compare different options to model the pseudo material and chose the best.

1 Introduction

During filling of the die at the startup of the extrusion process, the location and velocity of the flow front will have a great influence on the deformation of the die, especially in porthole dies. This deformation will affect the performance of the die in the rest of the process. Increasingly tighter requirements on complexity and geometric tolerances raise the demand for more insight in the deformations during the process. While an optimized extrusion process should create not more than 15% scrap, it is in everyday practice not uncommon to have a scrap rates over 25%.

2 Modeling Aluminium Extrusion processes

Using ALE/Eulerian FEM simulations Lof [10] showed that this type of FEM is very suitable to make predictions about exit velocity and extrusion force. Using ALE/Eulerian formulated FEM the process can be modeled without the expensive remeshing. Lof only simulated the steady state flow through the die. Using Eulerian description to simulate the filling requires a method that tracks the interface between air and aluminium, the flow front. In this paper we will focus on interface tracking techniques using a fixed mesh on which a pseudo- concentration function is defined and convected during simulation.

In 1986 Thompson introduced the pseudo-concentration method [11], [12] to track the flow front. Besides the material variables an extra pseudo-concentration variable C is convected through a fixed mesh during the simulation. If $C = 1$ material is present, when $C = 0$ no material is present and at $C = 0.5$ is the material-air interface. The discontinuity of the pseudo- concentration function around the flow front introduces inaccuracy during the convection through the FEM mesh. Dvorkin [4] already notices that if the initial distribution of the concentration function is smooth enough, no smoothing algorithm is necessary. Dvorkin chooses to reduce the viscosity with a factor 1000, if the concentration function is greater than zero. The boundary conditions are concentration function dependent, to prevent the effects of incompressibility of the material that gets trapped. Between the material and the boundaries. Incompressibility effects of the material the gets trapped inside its self are not taken care of.

3 Particle track method

As pseudo-concentration function we chose the initially smooth function of the original coordinates. The method is implemented in our In-house code DiekA. The original coordinate in integration point i is calculated as in equation 1 and the total displacement U is calculated in an ALE/EULERIAN formulation.

$$X_0^i = X^i - U^i \quad (1)$$

On the convective part of the total displacement global smoothing is applied. Therefore the original coordinates are convected through the mesh together with the displacement and every step the material stiffness is updated based on the original coordinates at the beginning of the step. The total domain is split in two parts, in an aluminium domain and an air domain. The domains are split by an original coordinate function which has a value in every point of the domain: ρ_{val} . The stiffness in an integration point is based on $\rho_{val}^i = X_{ini}^i - X_0^i$, with X_{ini} the location of the initial front. If $\rho_{val}^i < 0$ the integration point is in the air domain and the material stiffness needs to be reduced. How this is done is explained in the next section.

To avoid the incompressibility effect of the material permeable boundary conditions are used. When in an element one of the integration points is in the aluminium domain the contribution for all nodes to the stiffness matrix is in the order of the aluminium. Without permeable boundary conditions the domain would not fill completely. In a simulation this effect can be seen in layer of elements at the boundary which are filled for approximately 50%. Only using permeable boundary conditions however would be a problem as soon as air gets trapped inside the aluminium, which can happen if porthole dies are used and aluminium has to weld together after it has passed the legs. Therefore also the material in the air domain is adjusted so that is is compressible. In Fig. 1 is shown how the boundary conditions are updated every step based

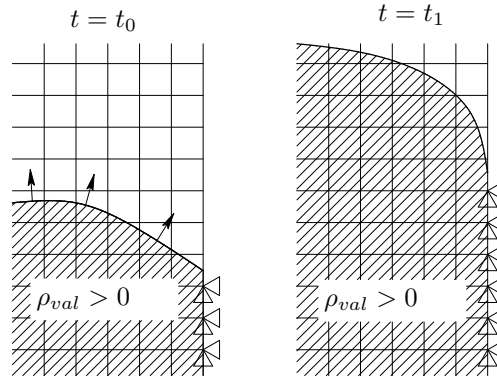


Figure 1: Permeable boundary conditions

on the value of ρ_{val}^n in the (boundary) nodes. The aluminium is modeled with the Sellers-Tegart Law:

$$\sigma_y = s_m \operatorname{arcsinh} \left(\left(\frac{\dot{\kappa}}{A} \exp\left(\frac{Q}{RT}\right) \right)^{\frac{1}{m}} \right) \quad (2)$$

In this equation $\dot{\kappa}$ is the equivalent plastic strain rate. The other parameters are constant during the simulation. Therefore the flow stress only depends on the equivalent plastic strain rate.

4 Modeling the pseudo material

The pseudo material can be modeled in many different ways. Here we explored 26 different models. In simulation 0 (see table 1) the pseudo material is modeled as a viscous material with a low viscosity to ensure enough stiffness reducing and a low bulk modulus to make the pseudo material compressible. In the other 25 simulations the material model for the pseudo material is the same as the aluminium model (equation 2). The stiffness reduction is done on different levels in DiekA. In figure 2 a simplified chart of the implementation of DiekA is given. The stiffness reduction can be done in either Predictor, Corrector or in both steps. The latter is

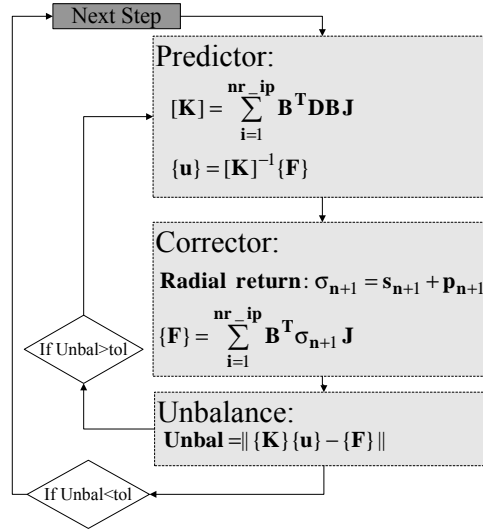


Figure 2: simplified incremental implementation

preferred because of conservation of consistency between predictor and corrector. In the input file in Dieka five multiplication factors can be defined. If in an integration point the OCTVAL is less than zero, the factors are applied in the following manner.

- ρ_{yld}
The factor ρ_{yld} is multiplied with the yield stress related to the equivalent strain rate as defined in equation 2. This impacts the material stiffness D used in the predictor step and the stress calculated in the radial return routine in the corrector step.
- ρ_{blk}
The factor ρ_{blk} is multiplied with the bulk modulus. This also impacts the material stiffness D in the predictor step and it reduces the hydrostatic pressure part of the stress p in the corrector step.
- ρ_{sig}
The factor ρ_{sig} is multiplied only with the deviatoric stress s in the corrector step.
- ρ_{hyd}
The factor ρ_{hyd} is multiplied directly with the hydrostatic stress p in the corrector step.
- ρ_{det}
The factor ρ_{det} is multiplied with the determinant of the Jacobian J in both predictor when calculation the contribution of an integration point to the stiffness matrix $[K]$ and the corrector step in the calculation of the Force vector in the corrector step.

Table 1: Simulations

Simulation	ρ_{yld}	ρ_{blk}	ρ_{sig}	ρ_{hyd}	ρ_{det}	run
0	Viscous,	$\mu = 1e - 6m^2s^{-1}$,	$C_b = 1MPa$			OK
1	0.1	1.0	1.0	1.0	1.0	Incomplete
2	0.01	1.0	1.0	1.0	1.0	Fails
3	0.001	1.0	1.0	1.0	1.0	Fails
4	1.0	0.1	1.0	1.0	1.0	OK
5	1.0	0.01	1.0	1.0	1.0	OK
6	1.0	0.001	1.0	1.0	1.0	OK
7	0.01	0.01	1.0	1.0	1.0	Incomplete
8	0.01	0.001	1.0	1.0	1.0	OK
9	0.01	0.00001	1.0	1.0	1.0	Fails
10	1.0	1.0	1.0	1.0	0.1	OK
11	1.0	1.0	1.0	1.0	0.01	Incomplete
12	1.0	1.0	1.0	1.0	0.001	Incomplete
13	1.0	1.0	0.667	1.0	1.0	OK
14	1.0	1.0	0.333	1.0	1.0	OK
15	1.0	1.0	0.000	1.0	1.0	Fails
16	1.0	1.0	-0.333	1.0	1.0	Fails
17	1.0	1.0	-0.667	1.0	1.0	Fails
18	1.0	1.0	-1.000	1.0	1.0	Fails
19	1.0	1.0	1.0	1.0	1.0	OK
20	1.0	1.0	1.0	0.667	1.0	OK
21	1.0	1.0	1.0	0.333	1.0	OK
22	1.0	1.0	1.0	0.000	1.0	Fails
23	1.0	1.0	1.0	-0.333	1.0	Fails
24	1.0	1.0	1.0	-0.667	1.0	Fails
25	1.0	1.0	1.0	-1.000	1.0	Fails

5 Numerical Experiments

Simulations with plane strain and axially symmetric Q4 elements are performed. The aluminium is modeled isotropic with a Sellars-Tegart law. In the air domain different material models and numerical tricks are used to make its stiffness 2- 3 orders lower than the stiffness of the aluminium. The different options are described in table 1. Simulation 0 is with the pseudo material modeled as a viscous material.

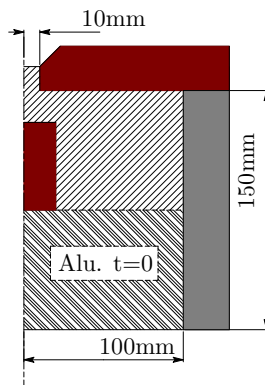


Figure 3: 2D geometry

In the rest of the simulations the air is modeled with the Sellers - Tegart law adjusted as de-

scribed in the previous section with the factors as in the table. The geometry for the test is a 2D plane strain model see figure 3. The single crosshatched section is the domain inside the die filled with air at the start of the simulation. The double crosshatched section is the domain inside the container already filled with aluminium. The container and die walls are assumed sticking, except for the bearing where frictionless slip is assumed. Again, when no Aluminium is present the boundary conditions are released, therefore making the wall permeable for air. The isothermal simulation is performed at 823K. The system is solved with a direct solver with an unbalance tolerance of 0.001.

6 Results

The best option will be chosen based on the results on volume conservation, flow front shape, ability to fill corners and the simulation times. First the simulations that had a step that didn't converge were ignored. In figure 4 the simulation times of completed simulations are shown.

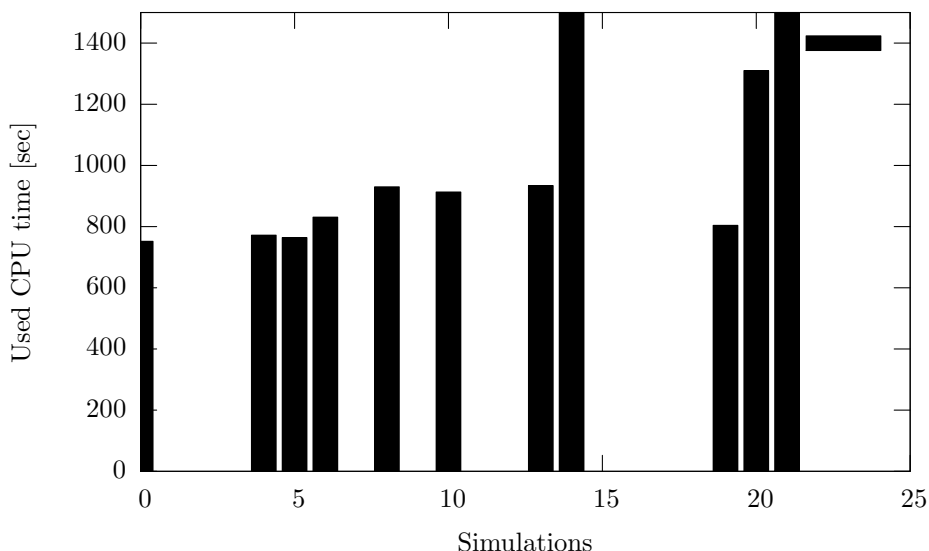


Figure 4: Used CPU time per simulation

The simulation with the pseudo-material modeled with a viscous material converges properly. Simulation 1 does run, but only until step 1524. This is the point where the die is almost filled except for the bearing and "welding chamber". Simulations 2, 3, and 9 reach the maximum iterations at the first step. The same thing happens for simulation 15 to 18 and 22 to 25. The bad convergence behavior of these simulations can be easily explained by the fact that only in the corrector step the stresses are updated according to the *OCTVAL*. Simulation 19 is the reference simulation in which all the factors are 1.0, meaning that both air and aluminium are modeled as aluminium. In simulation 20 & 21 the hydrostatic stress is affected only mildly, so the consistency between predictor and corrector is not disturbed to badly, but convergence is slow and time consuming.

However the flow front is also not different from the flow front in simulation 19 as can be seen in figure 5. Only simulation 0 and simulation 8 give a good representation of the flow front. Simulation 11 also gives the same flow front, however this simulation only runs up to step 923 and will therefore be ignored. In the figure 6 the volume conservation is plotted against the

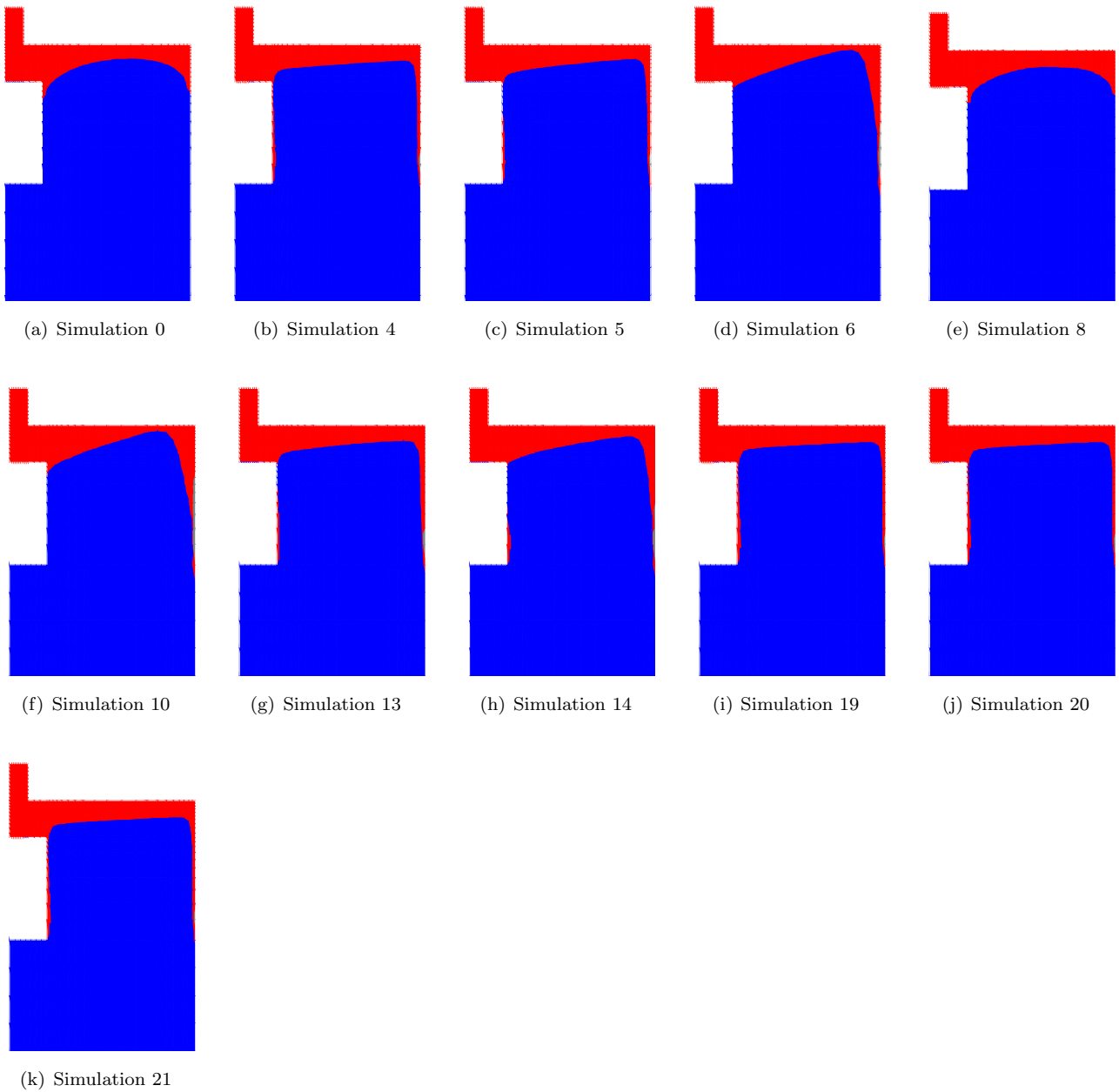


Figure 5: Flow front shapes

steps. Only simulation 0, 8 and 19 are plotted.

The oscillations in the beginning of the simulations can be explained by the behavior of the under integrated 4 nodes bilinear elements. At the walls the filling is far from smooth. First filling lags behind in these elements then in a few steps the elements fills completely. This effect is a combination of the permeable boundary conditions and the element that has no stabilization against spurious modes from the under integration. This leads to the non physical stick- slip behavior at the wall. Besides that it can be concluded that all the simulation are accurate in volume conservation.

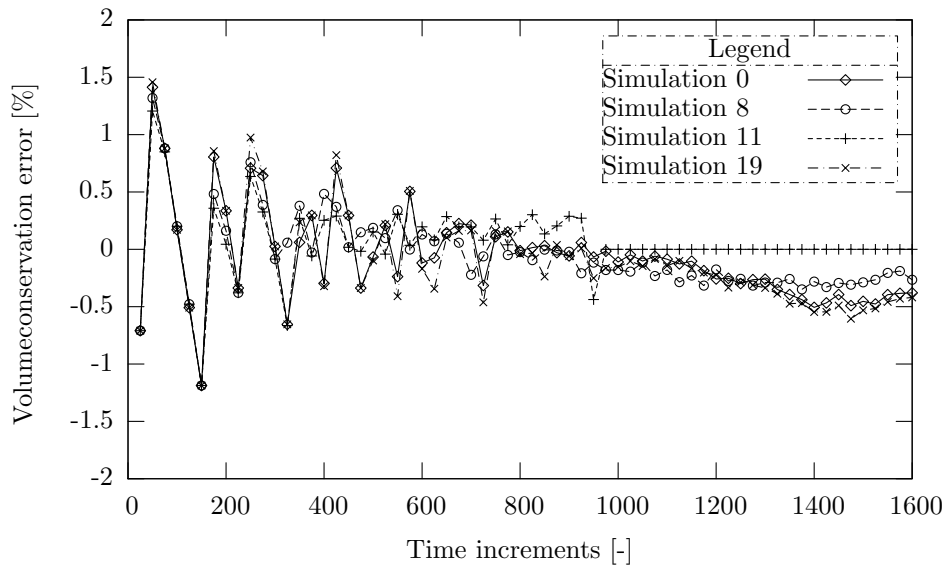


Figure 6: Volume conservation

7 Discussion

In this paper we show that the Particle track method is suitable to make efficient simulations of the filling of the dies. The volume conservation is accurate and the flow front looks good, however no comparisons with experiments have been made yet. Besides that a stabilization should be applied for this element to prevent the oscillatory behavior. Based on the results shown the method will be implemented for 3D simulations and simulations of aluminum flow in porthole dies can be performed.

References

- [1] Cavaliere, M. A., M. B. Goldschmit, et al. (2001). "Finite element analysis of steel rolling processes." *Computers & Structures* 79(22-25): 2075-2089.
- [2] Cruchaga, D. C., Tezduyar, T.E., (2002). "Computation of mould filling processes with a moving Lagrangian interface technique." *Communications in Numerical Methods in Engineering* 18(7): 483-493.
- [3] Devals, C., Heniche, M., Bertrand, F., Hayes, R. E., Tanguy, P. A., (2005). "A finite element strategy for the solution of interface tracking problems." *International Journal for Numerical Methods in Fluids* 49(12): 1305-1327.
- [4] Dvorkin, E. N., Petöcz, E.G. (1993). "An effective technique for modeling 2D metal forming processes using an Eulerian technique." *Engineering Computations* 10(4): 323-336.
- [5] Dvorkin, E. N., Cavaliere, M. A., et al. (1995). "A three field element via Augmented Lagrangian for modeling bulk metal forming processes." *Computational Mechanics* 17(1-2): 2-9.
- [6] Dvorkin, E. N., Goldschmit, M. B., et al. (1997). "2D finite element parametric studies of the flat-rolling process." *Journal of Materials Processing Technology* 68(1): 99-107.
- [7] Dvorkin, E. N., Toscano, R. G. (2003). "A new rigid-viscoplastic model for simulating thermal strain effects in metal-forming processes." *International Journal for Numerical Methods in Engineering* 58(12): 1803-1816.
- [8] Haagh, G., Van De Vosse, F. N. (1998). "Simulation of three-dimensional polymer mould filling processes using a pseudo-concentration method." *International Journal for Numerical Methods in Fluids* 28(9): 1355-1369.

- [9] Lewis, R. W., Ravindran, K. (2000). "Finite element simulation of metal casting." *International Journal for Numerical Methods in Engineering* 47(1-3): 29-59.
- [10] Lof, J. (2000). "Developments in finite element simulations of aluminium extrusion." PhD Thesis, University of Twente, Enschede.
- [11] Thompson, E. (1986). "Use of Pseudo-concentrations to follow creeping viscous flows during transient analysis." *International Journal for Numerical Methods in Fluids* 6(10): 749-761.
- [12] Thompson, E. (1988). "Transient analysis of forging operations by the pseudo-concentration method." *International Journal for Numerical Methods in Engineering* 25(1): 177-189.
- [13] Tezduyar, T.E. (2006). "Interface-tracking and interface-capturing techniques for finite element computation of moving boundaries and interfaces." *Comput. Methods Appl. Engrg.*, Vol. 195 (2006), 2983-3000